SIMULATING MALPASSET (FRANCE) DAM-BREAK CASE STUDY BY A TWO-DIMENSIONAL SHALLOW FLOW MODEL

Le Thi Thu Hien[1], Ho Viet Hung[1]

Abstract: *The paper is dedicated to researching a numerical model for dam-break simulation, which is verified through a comparison between calculated results and observed data of two reference tests. The numerical model is applied to simulate the flooding wave for the Malpasset dam-break event, which occurred in southern France in 1959. This event is a unique opportunity for code validation due to the availability of extensive field data on the flooding wave. In this research, Finite Volume Method (FVM) is applied to solve Two-Dimensional Shallow Water Equations (2D SWE) on structured mesh. Also, flux difference splitting method is utilized to construct numerical solvers of SWE.*

Keywords: Finite Volume Method; Flux difference Splitting Method; Malpasset (France).

1. INTRODUCTION

Finite Volume Method is considered as the most applied numerical strategy to simulate most complicated shallow water flow phenomena, for instant: transcritical and supercritical flows, discontinuous type flow or moving wet/dry front, etc. Besides, the numerical simulation of natural case study is characterized by several problems, such as: complex geometry, high roughness coefficient. Dam-break problem over real geometrical irregularities and rough bottom is always a big challenge in simulating flood wave on downstream. Thus, a stable algorithm, can work with 2D meshes and provided with shock-capturing ability is needed (Valiani et al, 2002). The effectiveness and robustness demonstrated by comparing numerical results with observed ones of the reference test cases, indicating good application aspects is an important goal of this project. A well-known test case Malpasset (France) which has experiment data is applied to obtain hydraulic characters: water hydrographs, maximum water level or arrival time at survey points and inundation maps at certain time.

[1] *Thuyloi University.*

2. NUMERICAL MODEL

2.1. Governing mathematical scheme

The conservation form of 2D SWE can be written as (Cunge et al, 1980):

$$\frac{\partial U}{\partial t}+\frac{\partial K(U)}{\partial x}+\frac{\partial H(U)}{\partial y}=S_1(U)+S_2(U) \quad (1)$$

In (1), **U** is the vector of conserved variables; **K** and **H** are flux vectors; $\mathbf{S_1}$ and $\mathbf{S_2}$ are bed slope term and friction term.

$$U=\begin{bmatrix} h \\ hu \\ hv \end{bmatrix};\ K(U)=\begin{bmatrix} hu \\ hu^2+0.5gh^2 \\ huv \end{bmatrix};\ H(U)=\begin{bmatrix} hv \\ huv \\ hv^2+0.5gh^2 \end{bmatrix} \quad (2)$$

$$S_1(U)=\begin{bmatrix} 0 \\ -gh\frac{\partial z_b}{\partial x} \\ -gh\frac{\partial z_b}{\partial y} \end{bmatrix};\quad S_2(U)=\begin{bmatrix} 0 \\ -\frac{\tau_x}{\rho} \\ -\frac{\tau_y}{\rho} \end{bmatrix}, \quad (3)$$

in which τ_x and τ_y are bottom shear stress given by:

$$\tau_x=\rho C_f u\sqrt{u^2+v^2};\ \tau_y=\rho C_f v\sqrt{u^2+v^2};\ C_f=\frac{g.n^2}{h^{1/3}} \quad (4)$$

where: h is flow depth, u and v are the velocity components in x and y directions. z_b is bottom elevation; n is Manning roughness coefficient; g is the acceleration due to gravity.

2.2. Numerical scheme

The flow variables are updated to a new time step by the Eq. 5, based on Godunov type,

$$\mathbf{U}_{i,j}^{n+1} = \mathbf{U}_{i,j}^{n} - \frac{\Delta t}{\Delta x}\left[\mathbf{K}_{i+1/2,j} - \mathbf{K}_{i-1/2,j}\right] - \frac{\Delta t}{\Delta y}\left[\mathbf{H}_{i,j+1/2} - \mathbf{H}_{i,j-1/2}\right] + \Delta t\mathbf{S}_{1i,j} + \Delta t\mathbf{S}_{2i,j} \qquad (5)$$

where superscripts denote time levels; subscripts i and j are space indices along x and y directions; Δt, Δx, Δy are time step and space sizes of the computational cell.

Flux Difference Splitting method is proposed by (Hubbard et al, 2000), which construct numerical solvers of SWE. The discretisation is performed so that retains an exact balance between flux gradients and source terms; Roe scheme is selected for approximation flux terms.

Hence, the final numerical solution obtained by this scheme is represented in (6),

$$\begin{aligned} \mathbf{U}_{i}^{n+1} &= \mathbf{U}_{i}^{n} - \frac{\Delta t}{\Delta x}\left(\mathbf{K}_{i+1/2,j} - \mathbf{K}_{i-1/2,j}\right) - \frac{\Delta t}{\Delta y}\left(\mathbf{H}_{i,j+1/2} - \mathbf{H}_{i,j-1/2}\right) \\ &+ \Delta t(\mathbf{S}^{+}_{1x(i+1/2,j)} + \mathbf{S}^{-}_{1x(i-1/2,j)}) + \Delta t(\mathbf{S}^{+}_{1y(i,j+1/2)} + \mathbf{S}^{-}_{1y(i,j-1/2)}) + \Delta t \cdot \mathbf{S}_{2} \end{aligned} \qquad (6)$$

2.3. Wet/dry front treatment

Roe method does not yield the correct flux at a boundary between a wet and dry cell (Bradford and Sanders, 2002). In finite volume based SW models, moving boundaries are considered as wet/dry fronts and hence included in the ordinary cell procedure in a through calculation that assumes zero water depth for the dry cells. A cell is considered dry if the water depth in the cell is below threshold value. A numerical technique based on the discrete form of the mass conservation equation which preserved steady state at the wet/dry front over was proposed by Brufau et al. (2002) to avoid difficulties in correspondence of adverse slopes.

According to Brufau et al. (2002), a proper way to deal with this problem is represented by Fig. 1. In order to avoid numerical error, local redefinition of the bottom level difference at the interface is enforced to fulfill the mass conservation equation.

$$z_{bR}^{\mathrm{mod}} = z_{bL} - \left(h_R - h_L\right) \qquad (7)$$

where z_{bR} is bottom elevation on the right cell; z_{bR}^{mod} is modified bottom; h_L and h_R are water depth on the left and the right cells as presented on the Fig. 1.

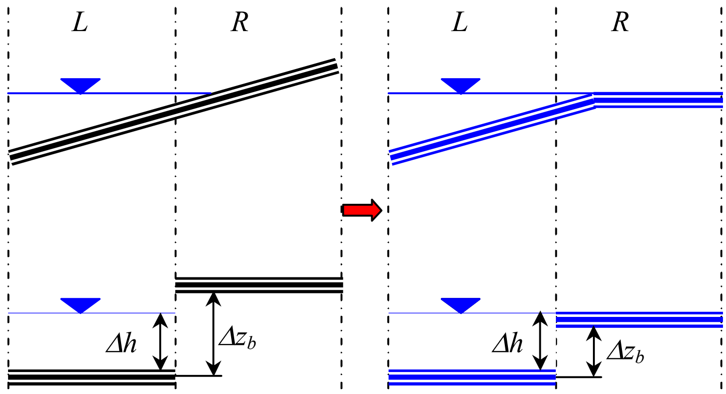

Fig. 1. Modification of the bed slope in steady wet/dry fronts over adverse steep slopes in real and discrete representations (Brufau et al., 2002).

The test case sketched in Fig. 2 demonstrates the effectiveness of the above treatment. The domain contains two islands, one of which is fully submerged while another one is partially submerged. The elevation of water is remained at rest 0.152*m* and discharge is set equal 0.0. Obviously, without treatment of wet/dry front the numerical solution is unphysical.

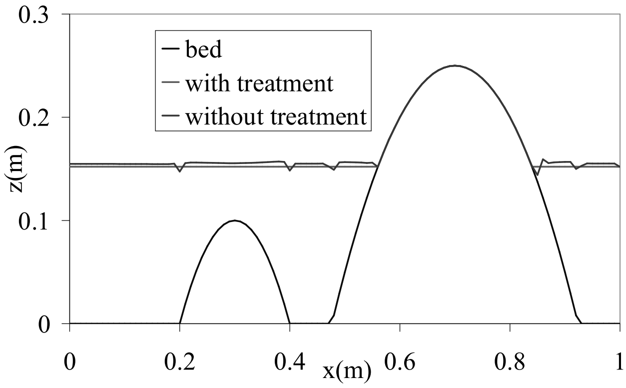

Fig. 2. Numerical solutions with and without wetting/drying front treatment.

The proposed numerical model is written by Fotran 90 language. Several test cases with analytical or empirical results are simulated to validate it (Le, 2014). Such challenges in working with numerical model such as: oscillation unphysical result, satisfied C-property or good tracking wet, dry fronts... are verified that this numerical model can be applied to a real case study – Malpasset (France) which has complex bathymetry and topography.

3. VALIDATION

3.1. Total dam-break flow over triangle obstacle

One of the famous tests mentioned (see its configuration in Fig. 3) is provided by the Laboratory of Researches Hydraulics of Chatelet and the Free University of Bruxelles (Belgium). The width of channel is 1.0*m*, water depth in reservoir is 0.75*m* and total length of channel is 38.0*m*. The height of obstacle is 0.4*m*. Manning coefficient *n* is set equal to 0.0125$sm^{-1/3}$. For the simulation, the computational domain is divided by a uniform grid of 0.1*m* resolution and the computational time is 40*s*. Reflective boundary conditions are used at the upstream end and two lateral sides of the domain, while transmissive condition is imposed at the downstream end.

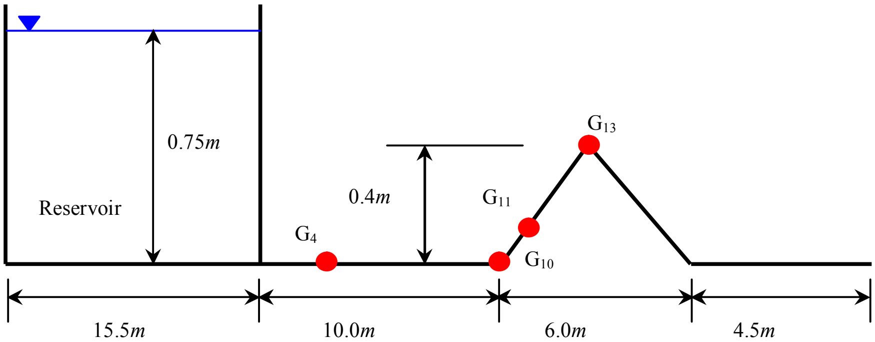

Fig. 3. Sketch of test case of flow over triangular obstacle

Firstly, the computational results of water surface profiles at different times are shown in Fig. 4. These solutions are quite close with the same ones published in (Kuiry et al, 2012) and (Guan et al, 2013).

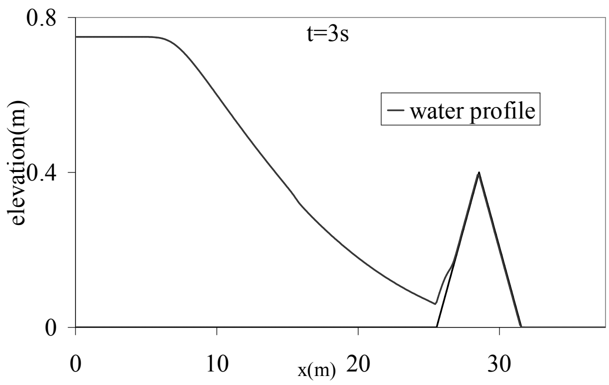

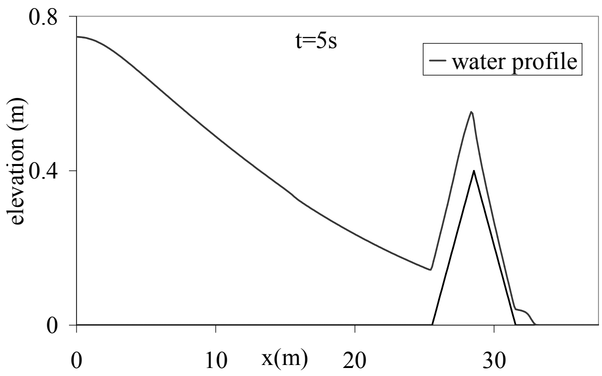

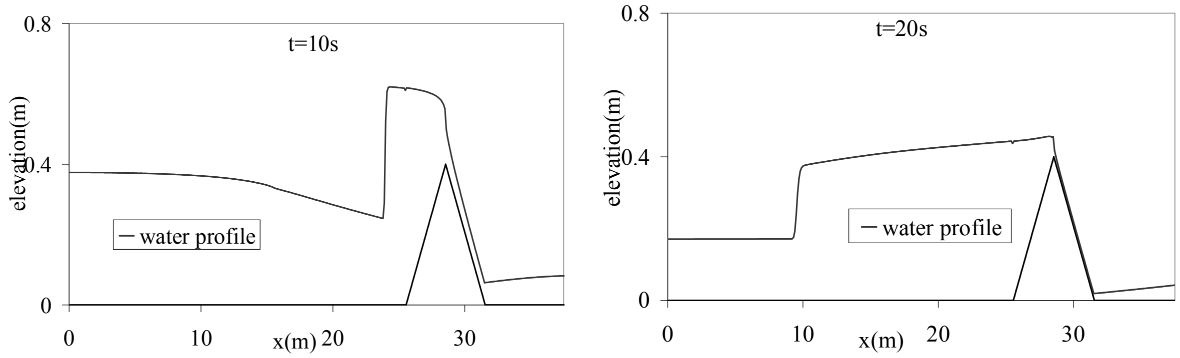

Fig. 4. Water surface profiles at difference times: t = 3s; t = 5s; t = 10s; t = 20s.

Secondly, the numerical solutions of water hydrographs obtained by the proposed scheme at different gauges G_4, G_{10}, G_{11}, G_{13} are indicated in Fig. 5. The comparison shows that the predictions of arrival time and water depth have good agreement with measurement data at gauges G_4, G_{10}, G_{11}. However, at gauge G_{13} (the crest of obstacle), a discrepancy of water depths of numerical solutions and experiment data appears, but the arrival time is still well-predicted.

The Nash-Sutcliffe model efficiency coefficient (E) is used to quantitatively describe the accuracy of model outputs for water depth at different study points by equation (8):

$$E = 1 - \frac{\sum_{i=1}^{n}\left(X_{obs,i} - X_{model}\right)^2}{\sum_{i=1}^{n}\left(X_{obs,i} - \overline{X_{obs}}\right)^2} \qquad (8)$$

where X_{obs} is observed values and X_{model} is modeled values at time *i*.

The Nash values at gauges G_4; G_{10}; G_{11} and G_{13} are 88.2%; 95.1%; 94.4% and 60.04%, respectively. It shows the above conclusion is correct

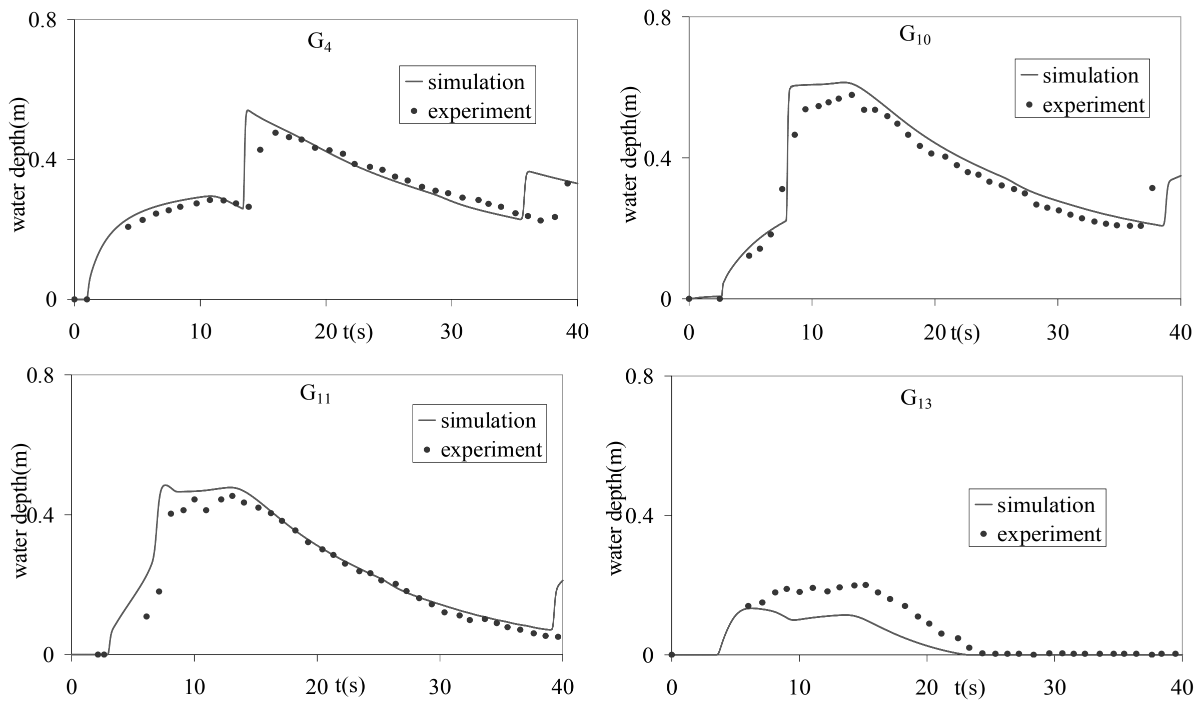

Fig.5. Water hydrographs at different sections: G_4, G_{10}, G_{11}, G_{13}

3.2. Partial dam-break flow over horizontal floodable area

(Aureli et al, 2011) also presented an experiment data of dam-break flow over horizontal floodable area. Initial water depths in the reservoir and downstream of the gate are 6.3*cm* and 1.27*cm* - 1.57*cm,* respectively. The initial water depth at the six gauge locations is slightly different (about 3*mm*) due to the deformation of the bottom of the experimental device, which was accurately measured and taken into account (see Fig. 6).

In the numerical simulation, Manning coefficient n is 0.007$sm^{-1/3}$ and a grid size $\Delta x=\Delta y=5mm$ is used. The computational time is set equal to 20*s* while the threshold value of water depth is 0.0004*m.*

Fig. 7 indicates water hydrographs at 6 study points. Globally, numerical result can capture well the trend of experimental hydrographs in all observed gauges. Especially arrival time to all the study points is very well captured (Fig. 7). For instant, Fig 8 is zoom out of 5 seconds first of water hydrographs at gauges G_3 and G_6. A remarkable good matching between computed and measured arrival times to the different gauges is also observed in this figure.

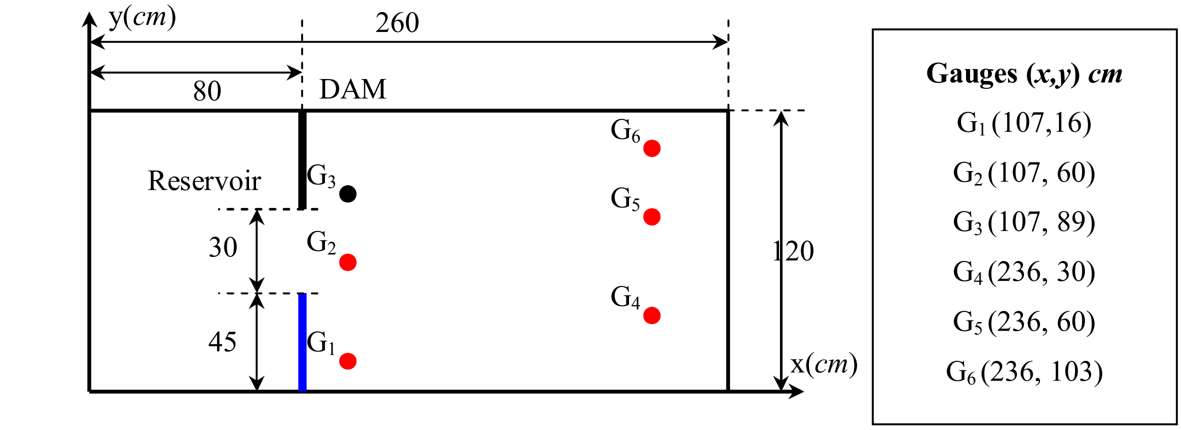

Fig. 6. Configuration of experiment test (dimension in cm).

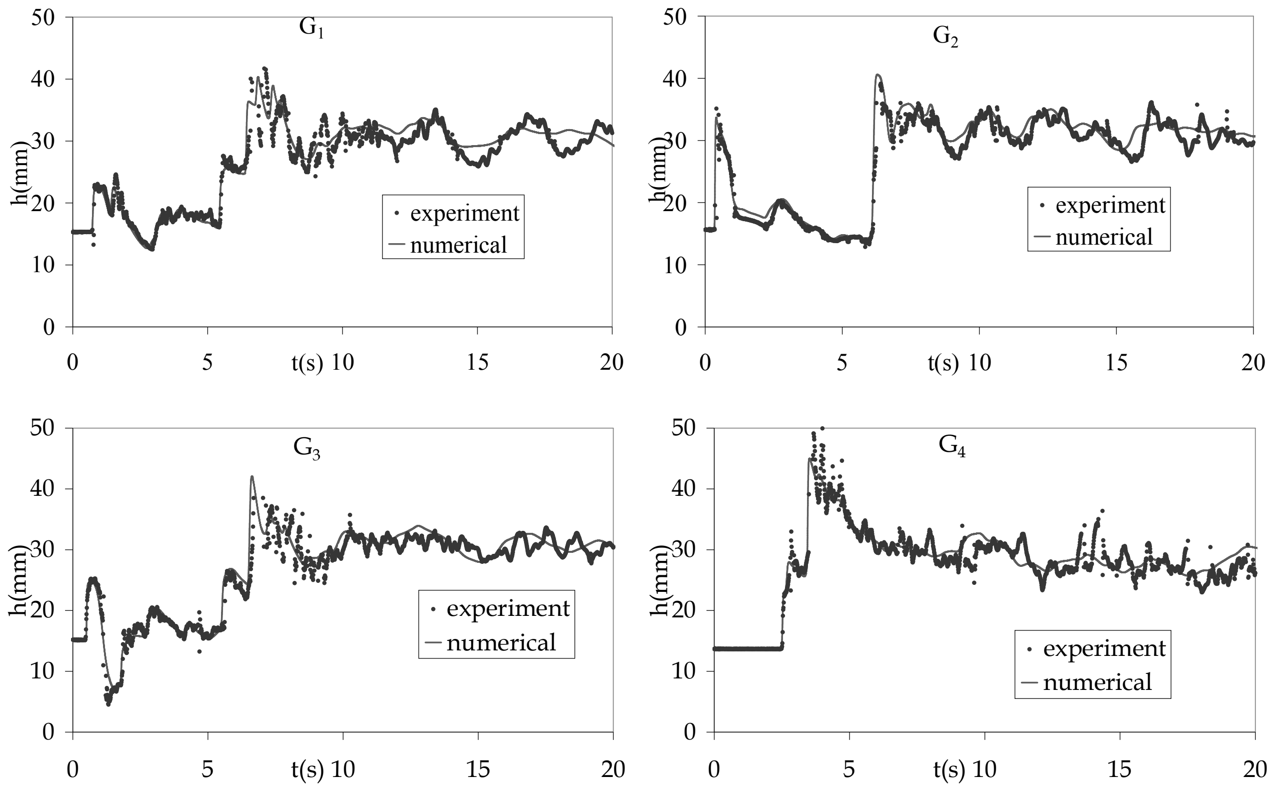

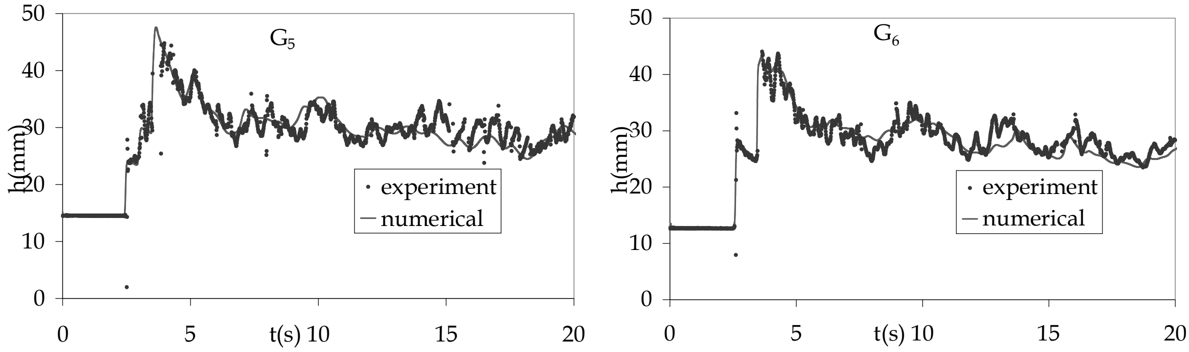

Fig. 7. Water hydrographs at 6 gauges: G_1; G_2; G_3; G_4; G_5; G_6

The Nash values at 6 gauges G_1; G_2; G_3; G_4; G_5; G_6 are: 90.5%; 87.46%; 94.08%; 89.82%; 84.0% and 89.77%, respectively. A very close agreement between experiment data and numerical solution is indicated. Thus, the proposed model is quite effective and robust in simulating dam break flow.

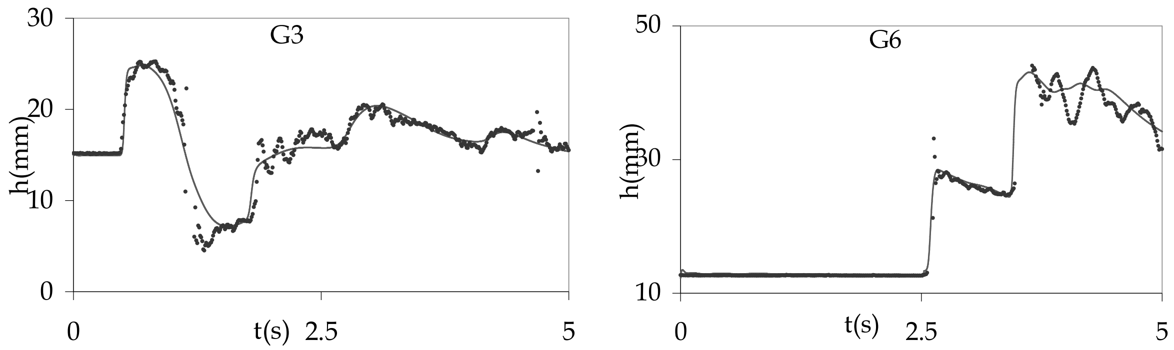

Fig. 8. Well-capture shock wave at gauges G_3 and G_6

4. APPLICATION

In order to validate the capability of the presented model in simulating dam break flows referring to field-scale case studies, the well-known test case of Malpasset (France) is taken as a reference test. Actually, observed data as well as experimental results obtained by physical modeling are available for this dam break event. The Malpasset Dam was located at a narrow gorge of the Reyran River valley with water storage of $55\times10^6 m^3$ and had a 66.5m high arch dam with a crest length of 233m. The dam failure occurred during the night of 2nd December 1959 because of heavy rain in the preceding days. A total of 433 casualties were reported.

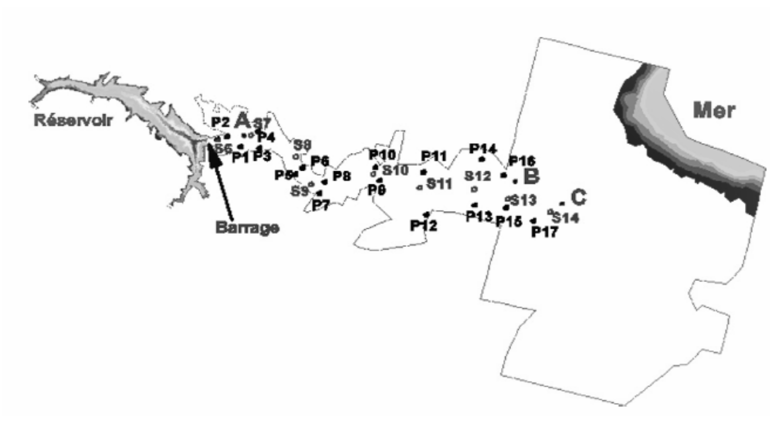

Fig. 9. Location of survey points (Shi et al, 2013)

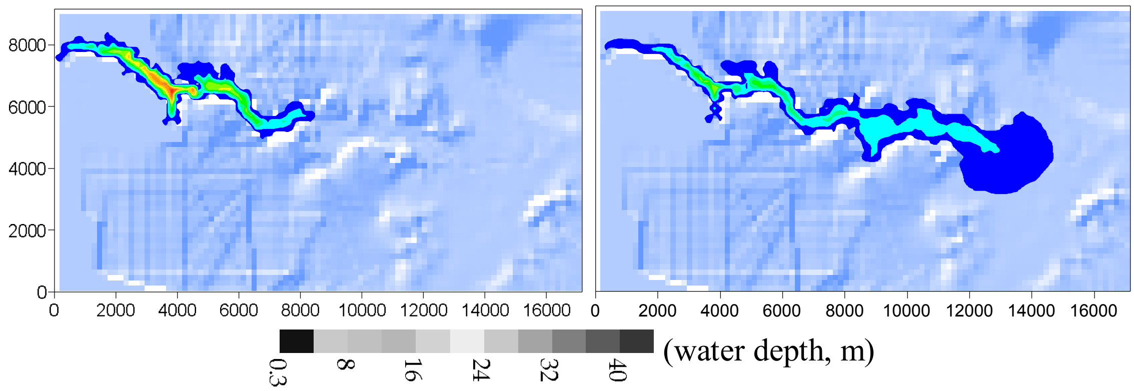

Fig. 10. Predicted inundation maps at different times: 600s and 2400s

The initial water elevation is set equal to +100.0*m a.s.l.* The elevation of valley floor ranges from -20.0*m* to +107.0*m a.s.l.* Except in the reservoir and in the sea, the bottom is considered dry although the outlet gate was opened. The Manning coefficient is set to $0.033sm^{-1/3}$.

In this study, the 17200*m* × 9200*m* computational domain is divided by a uniform mesh with 430×230 cells, corresponding to grid size $\Delta x=\Delta y=40m$. The threshold water depth h_ε is set up $10^{-4}m$ to define wet, dry cell.

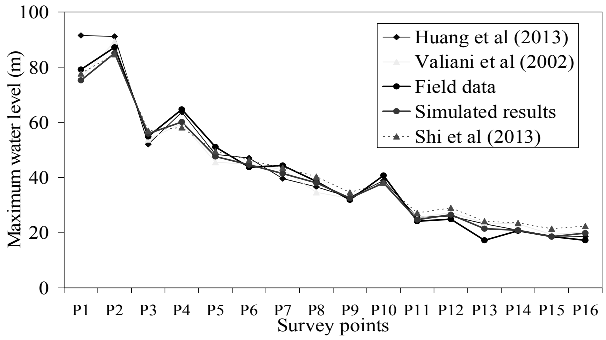

Fig. 11. Maximum water elevation at policy survey points

Fig. 10 shows water depth and flooding extents at t = 600*s* and t = 2400*s* computed by presented scheme. Meanwhile, Fig. 11 compares the predicted maximum water elevations at given study points (see their positions in Fig. 9) with those obtained by policy survey and other numerical results taken from (Huang et al, 2013), (Shi et al, 2013) and (Valiani et al, 2002). A good agreement is observed at all survey points.

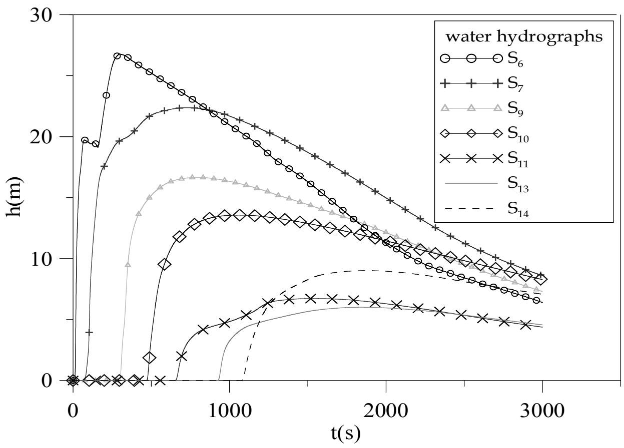

Fig. 12. Water hydrographs at policy survey points.

Figure 12 illustrates water hydrographs at different gauges, and indicates the numerical results of arrival time to these points. The close agreement can be seen between predicted solutions with experiment data and other numerical solutions in the Fig. 13. At points S_{10} and S_{13}, numerical errors are +8.4% and -3.5%, respectively, better than Shi's results (+12.9% and -5.76%). However, the opposite trend is shown at point S_9 (+15.2% in comparison with +7.6%).

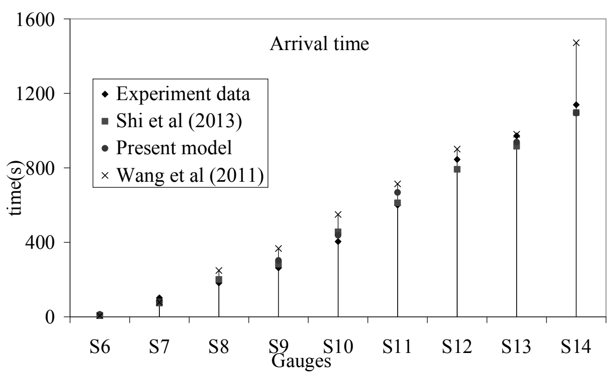

Fig. 13. Arrival time of the wave front at gauges in physical model

5. CONCLUSIONS

In this work, FVM is selected to solve 2D-SWEs on Cartesian mesh, FDS method is utilized to remain exactly balance between flux gradients and source terms. By two tests presented in this paper, the scheme demonstrated to behave satisfactorily with respect to their effectiveness and robustness in simulating total and partial dam-break flow over complex topographies, which can be able to work with real case study. The dam-break flood flow from Malpasset reservoir (France) is simulated by using presented model to obtain outflow hydrograph and flooding map. The numerical solutions are quite close with others in different works. It can be seen that this model is an indispensable tool for calculating and simulating scenarios if a dam-break occurs.

REFERENCES

Aureli. F; Maranzoni. A; Mignosa. P; Ziveri. C (2011). "*An image processing technique for measuring free surface of dam break flows*". Exp Fluids. 50, 665-575.

Bradford. S.F and Sander. B (2002). "*Finite volume model for shallow water flooding of arbitrary topography*". Journal of Hydraulic Engineering (ASCE). 128(3), 289- 298.

Brufau. P; Vaquez Cendon M.E; Garica–Navarro. P (2002). "*A numerical model for flooding and drying of irregular domains*". Int. J. Numer. Meth. Fluids. 39, 247-275.

Cunge. J.A; Holly. F.M; Verwey. A (1980). "*Practical aspects of computational river hydraulics*". London: Pitman Publishing Limited.

Guan. M; Wright. N. G; Sleigh. P.A (2013). "*A robust 2D shallow water model for solving flow over complex topography using homogeneous flux method*". International Journal for numerical methods in fluids. DOI: 10.1002/fld.3795.

Hubbard. M.E and Garcia Navarro. P (2000). "*Flux difference splitting and the balancing of source terms and flux gradients*". Journal of Computational Physics. 165, 89–125.

Huang. Y; Zhang. N; Pie. Y (2013). "*Well balanced finite volume scheme for shallow water flooding and drying over arbitrary topography*". Engineering Applications of Computational Fluid mechanics. 7(1), 40 – 54.

Kuiry. S.N; Sen. D; Ding. Y (2012). "*A high resolution shallow water model using unstructured quadrilateral grids*". Computers & Fluids. 68, 16-28.

Le T.T.H (2014), "*2D Numerical modeling of dam break flows with application to case studies in Vietnam*", Ph.D thesis, University of Brescia, Italia.

Valiani. A; Caleffi. V and Zanni. A (2002). "*Case study: Malpasset Dam-break Simulation using a two dimensional finite volume method*". J. Hydraulic Engineering. 128(5), 460- 472.

Shi. Y. E; Ray. R.K; Nguyen. K.D (2013). "*A projection method based model with the exact C–property for shallow water flows over dry and irregular bottom with using unstructured finite volume technique*". Computers and Fluids. 76, 178–195.

Wang. Y (2011). "*Numerical Improvements for Large-Scale Flood Simulation*". Thesis of Doctor Philosophy of Newcastle University.

Tóm tắt:

MÔ PHỎNG SỰ CỐ VỠ ĐẬP MALPASSET (PHÁP) BẰNG MÔ HÌNH TOÁN DÒNG CHẢY SÓNG NƯỚC NÔNG HAI CHIỀU

Bài báo này nghiên cứu về việc xây dựng một mô hình toán để mô phỏng sự cố vỡ đập. Mô hình đã được kiểm định bằng cách so sánh kết quả tính toán với số liệu thực đo của hai thí nghiệm. Mô hình toán được sử dụng để mô phỏng dòng chảy lũ khi xảy ra sự cố vỡ đập Malpasset ở Pháp năm 1959. Đây là cơ hội hy hữu để kiểm định mô hình toán vì có đầy đủ các số liệu thực đo và thực nghiệm mô hình. Trong nghiên cứu này phương pháp thể tích hữu hạn đã được sử dụng để giải hệ phương trình sóng nước nông hai chiều trên lưới có cấu trúc. Ngoài ra, thuật toán phân chia thông lượng đã được ứng dụng để tìm lời giải số cho hệ phương trình sóng nước nông.

Từ khóa: Phương pháp thể tích hữu hạn; thuật toán phân chia thông lượng; Malpasset (Pháp).

BBT nhận bài: 25/5/2017

Phản biện xong: 22/6/2017